AD-A061 343 NAVAL OCEAN SYSTEMS CENTER SAN DIEGO CA F/G 20/14
ZONAL WINDS AS A GENERATING MECHANISM FOR THE IONOSPHERIC IRREG--ETC(U)
JUN 78 M R PAULSON
UNCLASSIFIED NOSC/TR-290 NL

END
DATE FILMED
-79
DDC

NOSC

(12) SC

(13) 32p.

LEVEL II

NOSC TR 290

Technical Report 290

(14) NOSC/TR-290

(6)

ZONAL WINDS AS A GENERATING MECHANISM FOR THE IONOSPHERIC IRREGULARITIES THAT CAUSE EQUATORIAL SCINTILLATION OF SATELLITE SIGNALS.

(10) M.R. Paulson

(11) 26 Jun[illegible]78

(9) Research and Development Report. Jan[illegible] - Jun[illegible]78

Prepared for
Office of Naval Research

Approved for public release; distribution unlimited

(16) RR0320 8 (17) RR0320801

NAVAL OCEAN SYSTEMS CENTER
SAN DIEGO, CALIFORNIA 92152

393 159

JSW

NAVAL OCEAN SYSTEMS CENTER, SAN DIEGO, CA 92152

AN ACTIVITY OF THE NAVAL MATERIAL COMMAND

RR GAVAZZI, CAPT, USN
Commander

HL BLOOD
Technical Director

ADMINISTRATIVE INFORMATION

The work reported herein was performed for the Office of Naval Research under 61153N, RR0320801, 532-MP34 over the period January to June 1978.

Released by
JH Richter, Head
EM Propagation Division

Under authority of
RR Gardner, Associate Head
Environmental Sciences Department

UNCLASSIFIED

SECURITY CLASSIFICATION OF THIS PAGE *(When Data Entered)*

REPORT DOCUMENTATION PAGE		READ INSTRUCTIONS BEFORE COMPLETING FORM
1. REPORT NUMBER NOSC TR 290	2. GOVT ACCESSION NO.	3. RECIPIENT'S CATALOG NUMBER
4. TITLE *(and Subtitle)* Zonal Winds as a Generating Mechanism for the Ionospheric Irregularities that cause Scintillation of Satellite Signals		5. TYPE OF REPORT & PERIOD COVERED Research and development January - June 1978
		6. PERFORMING ORG. REPORT NUMBER
7. AUTHOR(s) MR Paulson		8. CONTRACT OR GRANT NUMBER(s)
9. PERFORMING ORGANIZATION NAME AND ADDRESS Naval Ocean Systems Center San Diego, CA		10. PROGRAM ELEMENT, PROJECT, TASK AREA & WORK UNIT NUMBERS 61153N, RR0320801, 532-MP34
11. CONTROLLING OFFICE NAME AND ADDRESS Office of Naval Research Washington, D.C.		12. REPORT DATE 26 June 1978
		13. NUMBER OF PAGES 27
14. MONITORING AGENCY NAME & ADDRESS*(if different from Controlling Office)*		15. SECURITY CLASS. *(of this report)* Unclassified
		15a. DECLASSIFICATION/DOWNGRADING SCHEDULE

16. DISTRIBUTION STATEMENT *(of this Report)*

Approved for public release; distribution unlimited.

17. DISTRIBUTION STATEMENT *(of the abstract entered in Block 20, if different from Report)*

18. SUPPLEMENTARY NOTES

19. KEY WORDS *(Continue on reverse side if necessary and identify by block number)*

Satellite communication
Solar cycle
thermosphere
F-region
ionospheric turbulence
interferometry

20. ABSTRACT *(Continue on reverse side if necessary and identify by block number)*

The theory that thermospheric zonal winds generate the ionospheric irregularities that cause scintillation is examined. Good correlation between diffraction pattern drift velocities and scintillation intensities tends to support the theory, but night-to-night variation in this relationship suggests that other factors may be operative. Additional measurements are recommended.

DD FORM 1 JAN 73 1473 EDITION OF 1 NOV 65 IS OBSOLETE
S/N 0102-014-6601

UNCLASSIFIED

SECURITY CLASSIFICATION OF THIS PAGE *(When Data Entered)*

SUMMARY

PROBLEM

Compare information available in the literature on thermospheric zonal winds with information on the occurrence of equatorial ionospheric scintillation to look for a correlation between the two phenomena. Additionally to look for a correlation between scintillation intensity of satellite signals and the diffraction pattern drift velocity, using data from spaced-receiver measurements made in Guam in 1976 on Gapfiller/Marisat UHF and L-band signals. The objective of this study is to try to evaluate the theory that zonal thermospheric winds are the generating mechanism for the ionospheric irregularities that cause scintillation.

RESULTS

Zonal winds at F-region heights have been shown to exist, both indirectly, by means of models of global atmospheric density and pressure, and directly, by means of measurements of doppler shift in the nighttime air glow at the 6300 Å oxygen line. The diurnal variation of these zonal winds in equatorial regions shows a pronounced similarity to the nighttime variation of equatorial scintillation intensity. Seasonal and solar-cycle variations in zonal winds have not been investigated in enough detail, however, to make a very meaningful comparison with the seasonal and solar-cycle occurrence of equatorial scintillation.

Comparisons of scintillation intensities with diffraction pattern drift velocities show good correlation, suggesting that the irregularities in the ionospheric electron density that cause the scintillation may be generated by turbulence produced by zonal winds. Night-to-night differences in the dependence, however, would indicate that, while zonal winds may be a necessary condition for scintillation, other factors also contributing to the scintillation intensity must be identified as well.

RECOMMENDATIONS

With the occurrence and the intensity of equatorial scintillation increasing as solar activity increases, additional spaced-receiver measurements should be made at both UHF and L-band frequencies to get further comparison between diffraction pattern drift velocities and scintillation intensity. The L-band measurements would be particularly useful since the scintillation at these frequencies doesn't reach saturation as soon as that at UHF.

Neutral thermospheric temperatures should also be monitored to look for a correlation between scintillation intensity and nighttime thermospheric temperatures and between zonal winds and nighttime thermospheric temperatures.

The zonal component of the neutral wind could be measured using the doppler shift of the 6300-Å oxygen line technique. Thermospheric temperatures could be determined from the doppler broadening of that same line.

These techniques would require that the measurements be made in some equatorial location where cloud cover would not be a problem.

Satellite measurements of solar radiations and particles should also be examined for periods when these measurements are made to look for solar effects that might sustain the nighttime thermospheric temperature and also look for other contributions to the scintillation intensity.

CONTENTS

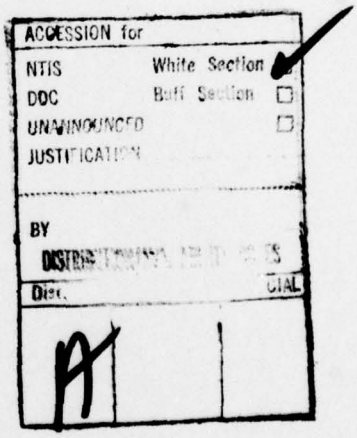

INTRODUCTION

Equatorial scintillation has been found to have, at times, a highly disruptive effect on UHF satellite communications of ships and communications stations in equatorial regions (Refs 1, 2). These effects can endure up to 5 hours and more per night, especially for periods around the equinoxes. Equatorial scintillation becomes progressively more intense and more frequent with increasing solar activity. Since a new solar cycle is starting and activity beginning to increase, the disruptive effects can be expected to increase in duration, intensity, and frequency of occurrence.

Although equatorial scintillation has been studied for many years no accepted theory has been developed to explain how the irregularities in electron density in the ionosphere, which cause the scintillation, are generated. If a generating mechanism can be identified it may be possible to predict when and where scintillation can be expected to occur.

Some results of a recent investigation of equatorial ionospheric scintillation of UHF satellite signals conducted by Naval Ocean Systems Center at the Naval Communication Area Master Station (NAVCAMS) in Guam suggest the possibility that the ionospheric irregularities may be generated by turbulence produced by zonal winds at ionospheric heights (Ref 2). The purpose of this report is to look at any information available in the literature on zonal winds and turbulence at ionospheric heights and how they vary diurnally and with solar activity and to try to evaluate feasibility of turbulence as a generating mechanism for ionospheric irregularities.

Additionally, the scintillation data taken on Guam in 1976 will be further processed to try to show a better correlation between the drift velocity and the scintillation intensity.

TURBULENCE THEORIES

Spaced-receiver measurements made at Jodrell Bank, England, in the early 1950's, using radio stars as signal sources (Ref 3), led Maxwell (Ref 4) to propose turbulence as a possible generating mechanism for the ionospheric irregularities which cause radio frequency scintillation. Using experimental data available at that time he estimated the Reyonlds number to be on the order of 300 for the F-region between 300 and 400 km and around 10^4 between 200 and 300 km. He states that, according to jet stream experiments, the critical value for the Reynolds number may be as low as 30. That is, for Reynolds numbers higher than this critical value, turbulence can be expected to occur. The Reynolds number is given as

$$\mathrm{Re} = \frac{\rho v \ell_o}{\mu}$$

where v is the velocity difference over a height, ℓ_o, μ is viscosity, and ρ is density.

The non-appearance of scintillation during the daylight hours is explained by Maxwell as being due to the inhibition of turbulence by large temperature gradients, by lower drift velocities, or by an increase in the kinematic viscosity. The appearance of scintillation, then, represents a transition from laminar flow during the daytime to non-laminar flow at night.

Dagg (Ref 5), who was also involved with the Jodrell Bank spaced-receiver measurements, disagrees with Maxwell's theory. According to Dagg, Maxwell's theory would require

a motion of the whole atmosphere at an altitude of 300 to 400 km, and the measurement of ionization drift would be a measurement of the total atmospheric drift velocity. Since velocity measurements were occasionally as high as 2000 m/sec, a velocity which greatly exceeds the speed of sound at that altitude, Dagg doesn't think that the total atmosphere could be drifting. Further, Dagg notes that a close correlation has been shown to exist between drift speed and changes in the earth's magnetic field, and it is not clear how changes in the earth's magnetic field can influence motions in the neutral air in the F-region. Dagg evidently doesn't consider the possibility of neutral winds influencing the magnetic field through the ionized material. Dagg's third objection to Maxwell's theory is that ionized material driven by zonal winds in the F-region would be strongly damped because of the earth's magnetic field and would not respond to the neutral winds.

In a companion paper Dagg (Ref 6) proposed a theory which attributes the generation of irregularities in the F-region to turbulent wind motion in the dynamo region at a height of 110 to 150 km. The turbulence is transferred to the F-region by the turbulent component of the electric potential field which is produced. It isn't clear how this theory explains, any more than Maxwell's, the high drift velocities that they measured.

In the original experiments of Maxwell and Dagg (Ref 3) it appears that many of their measurements were made using an east-west receiver spacing of 368 m and a north-south spacing of 315 m. This spacing would require very precise measurement of time differences for the high velocities that they report. Errors as small as a tenth of a second in time difference could result in large errors in velocity. The technique used to obtain time differences was that of matching similar fades. In this technique short sections of charts for pairs of receivers are slipped to line up similar fades and the time difference is measured. This technique is not very accurate for determining drift velocities when samll time differences are involved. Changes in the diffraction pattern as it drifts can shift the position of fades with respect to each other. These shifts, as well as short-time vertical components of drift, can indicate incorrectly high and low velocities. This may have produced the very high velocities that they measured.

Rishbeth (Ref 7) investigated the question of magnetic damping in the F-region for the equatorial case. Particular consideration was given to times around sunrise and sunset. He found that pressure gradients in the neutral air produce zonal winds, westward at sunrise and eastward at sunset. These winds produce vertical currents, which set up polarization fields. During the day these polarization fields are discharged through the E-layer. At night the E-layer is not sufficiently conducting so the polarization fields in the F Region build up and the plasma tends to move with the neutral wind.

THERMOSPHERIC WINDS

EVIDENCE FOR F-REGION NEUTRAL WINDS

Atmospheric drag is a major force affecting the period of a satellite at F-region heights. If the satellite orbit is sufficiently elliptical, most of the drag occurs at perigee. Changes in satellite period, then, can be used to determine atmospheric drag, and from those changes atmospheric densities can be obtained at or near perigee. Jacchia (Refs 8, 9) and Jacchia et al. (Refs 10, 11) used atmospheric drag on a large number of satellites to map global distributions of density and temperature at F-region heights for various solar and geomagnetic conditions. These distributions were used by various investigators to calculate global wind models at F-region heights.

Kohl and King (Ref 12) used Jacchia's (Ref 8) atmospheric model to calculate global wind systems in the upper atmosphere for various local times. Figure 1 is an example of their calculations for an altitude of 300 km and a peak electron density of 3×10^5 per cm^3 (sunspot minimum or night conditions). Figure 2 is for 10^6 electrons per cm^3 (sunspot maximum or daytime conditions). These calculations do not take into consideration a day-to-night variation in electron/ion density that would result in a diurnal variation in ion drag. This variation could modify their results. A combination of the night side of Fig. 1 with the day side of Fig. 2 might be more realistic. The times of maximum and minimum zonal winds would probably also be shifted.

Challinor (Ref 13) used an asymmetric pressure model, which he considered to be a more realistic model of upper air pressures. This model has maximum and minimum pressures at 1400 LMT and 0330 LMT, respectively, causing the isobars to be closer together around sunset than they are around sunrise. His work was also based on a pressure model developed by Jacchia and Slowey (Ref 14) but simplified for equinox conditions. He included the effects of ion motion, Coriolis, inertial and ion drag forces. Figure 3 is a plot of his results for 250 km. Challinor's results were in general agreement with experimental measurements, but he noted that the spatial resolution of the experimental results was too coarse for detailed comparison.

Blum and Harris (Refs 15, 16) have performed a full nonlinear treatment of the global thermospheric wind system. They considered horizontal motion of the neutral atmosphere between 120 and 500 km. A Jacchia (Ref 8) model atmosphere was used and, in addition, an ionospheric model by Nisbet (Ref 17). Steady-state conditions were assumed. That is, all variables such as density, temperature, viscosity, etc. were referred to a coordinate system that was fixed with respect to the sun. This means that each day of the year and each solar activity condition would produce a different wind model. Figures 4 and 5 are examples of calculated global wind fields at 300 km, one for equinox conditions and the other for northern summer solstice. For equinox conditions, the maximum global wind speed occurred around 2000 local time, with amplitudes ranging from 70 to 130 m/sec, depending on latitude. The precise solar conditions for these wind patterns were not stated, but in developing global patterns of the driving force which was used to get these winds, a solar 10.7-cm flux of 200 was used.

The preceding studies make various assumptions and simplifications that can affect the accuracy of the results in varying degrees. The original works should be consulted for details of the assumptions. All of the derivations, however, predict equatorial zonal winds with a diurnal variation and an eastward drift at night.

MEASURED THERMOSPHERIC WINDS

Most methods of determining thermospheric winds are indirect, such as the one discussed in the preceding section or that of Roble et al. (Ref 18) in which incoherent-scatter radar measurements of the diurnal variation of electron and ion temperatures, electron densities, and vertical plasma drifts were used to deduce velocities.

A direct measurement of thermospheric winds was made by Armstrong (Ref 19) using the Doppler shift in the 6300-Å oxygen line in the night air glow. The dissociative recombination of molecular oxygen ions in the region of the F2 maximum in the ionosphere is generally thought to be the origin of this emission.

Armstrong used a scanning photoelectric Fabry-Perot interferometer and recorded the emission alternately from two regions of the sky while scanning was in progress. The two sets of fringes obtained were then examined for any order shifts between them.

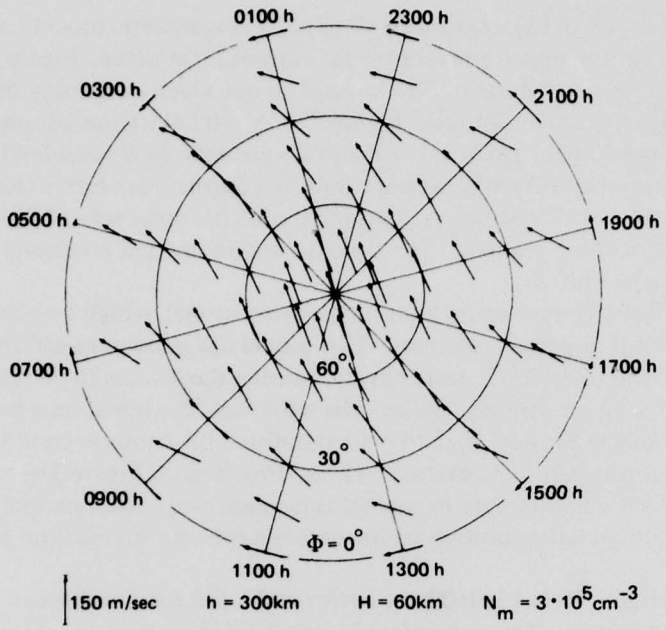

Figure 1. The atmospheric wind system in the northern hemisphere calculated for an altitude of 300 km when the peak electron density is 3×10^5 cm $^{-3}$. From Ref. 12.

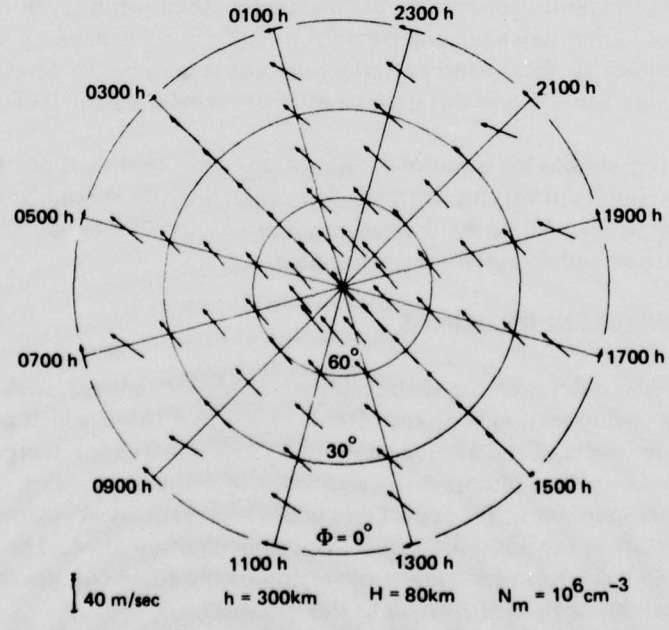

Figure 2. The a[illegible]ind system in the northern hemisphere calculated for an [illegible]00 km when the peak electron density is 10^6 cm^{-3}. From R[illegible]

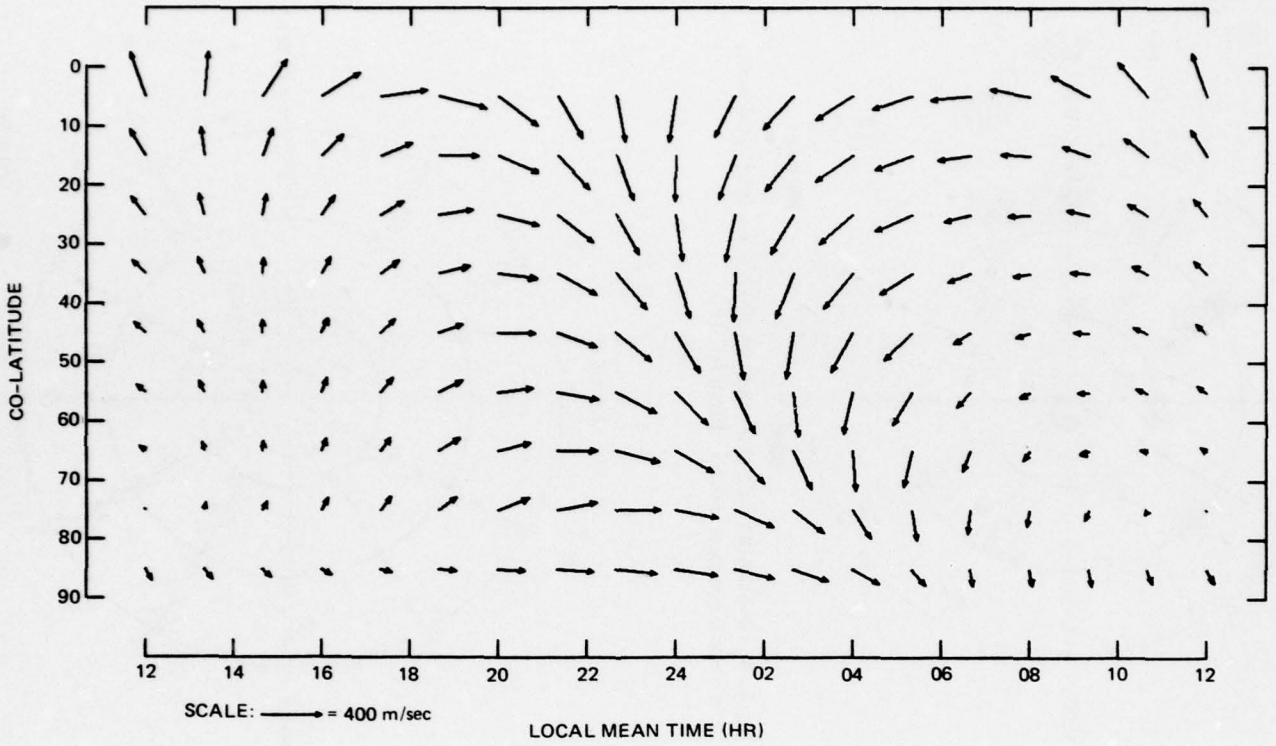

Figure 3. Predicted wind pattern at 250 km (Southern hemisphere is inferred by symmetry). From Ref 13.

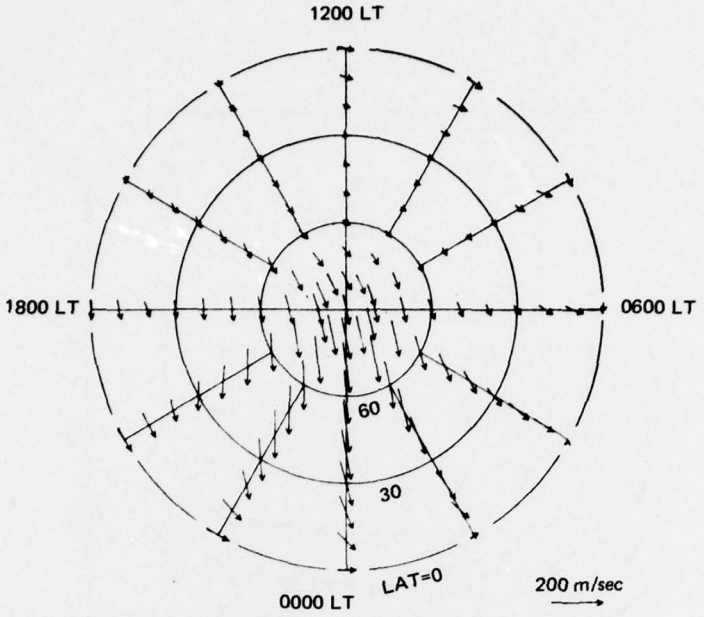

Figure 4. Global wind field at a height of 300 km, equinox conditions, Penn State ionospheric model. From ref. 15.

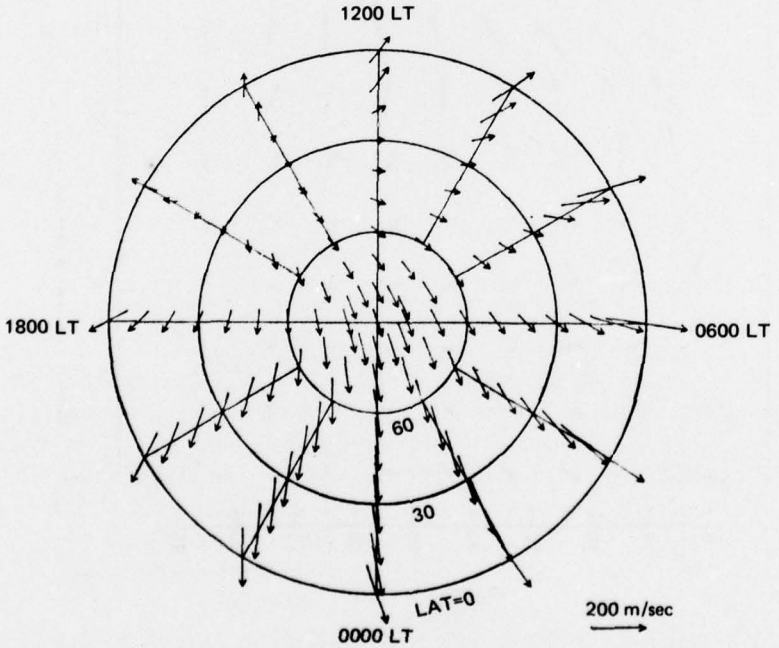

Figure 5. Global wind field for summer solstice conditions for the northern hemisphere. From Ref. 15.

If the two regions of the sky are chosen 180 deg apart in azimuth so that one direction is aligned with the thermospheric wind and the other is against it, the fringes recorded from one direction should indicate a velocity of approach and the other a velocity of recession. The difference between fringe shifts in the two directions then is a result of twice the velocity component along the line of sight. A steady velocity is required over a region of about 10 deg in latitude or longitude to allow low-elevation look angles. These low angles produce larger doppler shifts for greater system sensitivity. Armstrong estimated that wind speeds as low as 50 m/sec could be measured with his system to an accuracy of ±25 m/sec when the night glow was sufficiently intense. Figure 6 is an example of zonal winds measured at lat. 30.07° S, long. 209.33° W by means of this method. Figure 7 also shows some eastward velocities and equatorward velocities for individual nights. This location can be considered to be mid-latitude, and results here may be somewhat different from those in equatorial regions because of such factors as Coriolis force and the variation in solar heating with latitude.

Hernandez and Roble (Ref 20) also used a Fabry-Perot spectrometer at Fritz Peak Observatory (39.9° N, 105.5° W) to measure nighttime thermospheric winds and temperatures. The winds and temperatures were determined from the doppler shift and broadening of the 6300-Å oxygen line. The technique is similar to that used by Armstrong. However, they added a 2-Å rejection filter to remove any possible emission from the OH molecule, which could have produced errors in earlier work. Another improvement included in their equipment was a servo feedback technique to stabilize the interferometer, thus allowing longer measurement times. Because of the low emission rates, measurement times were on the order of 30 to 45 min for each direction. This allowed them to sample a given direction about every 2½ hours.

Measurements were made from November 1973 through February 1975, and data for quiet geomagnetic periods were separated from those for geomagnetically disturbed periods.

Hernandez and Roble separated their meridional and zonal wind measurements (Figs. 8 and 9, respectively) into three seasonal groups, summer, winter, and equinoctial. Meridional winds were found to be generally southward, with larger mean speeds in the summer of around 200 m/sec and winter speeds of less than 100 m/sec with occasional low northward winds occurring. The mean meridional winds were in general agreement with their calculated model.

Their zonal winds during the summer showed westward winds, while the winter months showed eastward winds. The equinoctial months showed winds changing from eastward to westward around local midnight. This is also in general agreement with their model except for the summer months. In this case their model showed that the zonal winds should have changed from eastward to westward around 0200 local time. This discrepancy, they say, may have resulted from the local time rate of change of the neutral atmosphere temperature being less than the model predicted during the summer months.

These measurements are also considered to be mid-latitude, but they do confirm the existence of zonal and meridional neutral winds and show general agreement with the global thermospheric wind patterns predicted from satellite drag measurements. It appears that the technique of measuring doppler shifts in the nighttime air glow to determine winds has not yet been used in equatorial regions. Possibly the extensive cloud cover common in much of that region would make such measurements difficult.

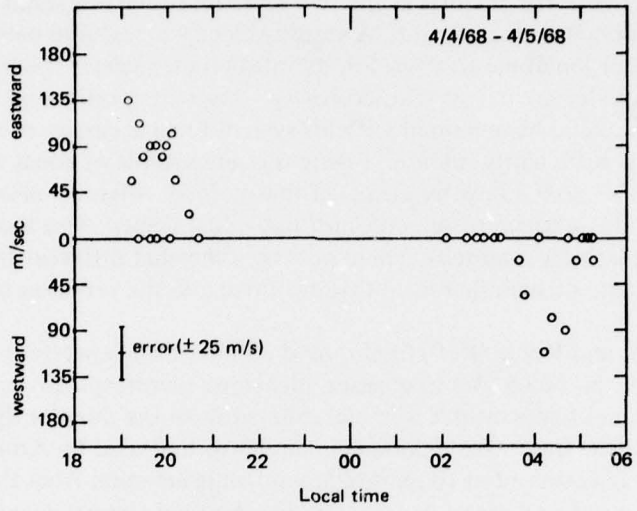

Figure 6. Eastward evening and westward morning winds for the period 4/4/68–4/5/68. From Ref. 19.

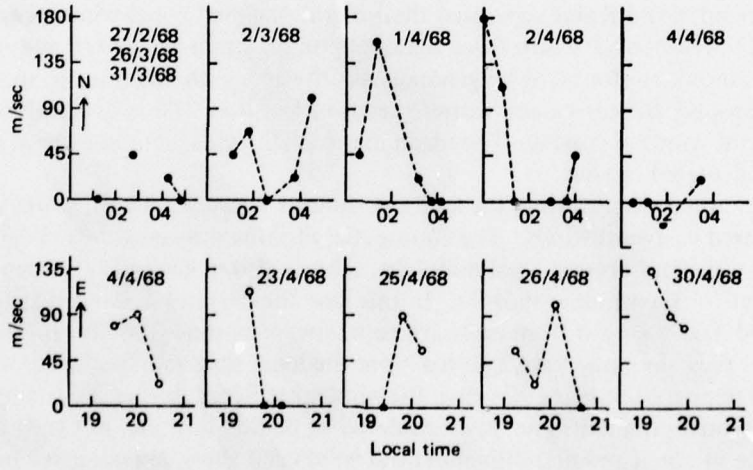

Figure 7. Records of equatorward winds on individual nights (top row) and eastward winds on separate evenings (bottom row). From Ref. 19.

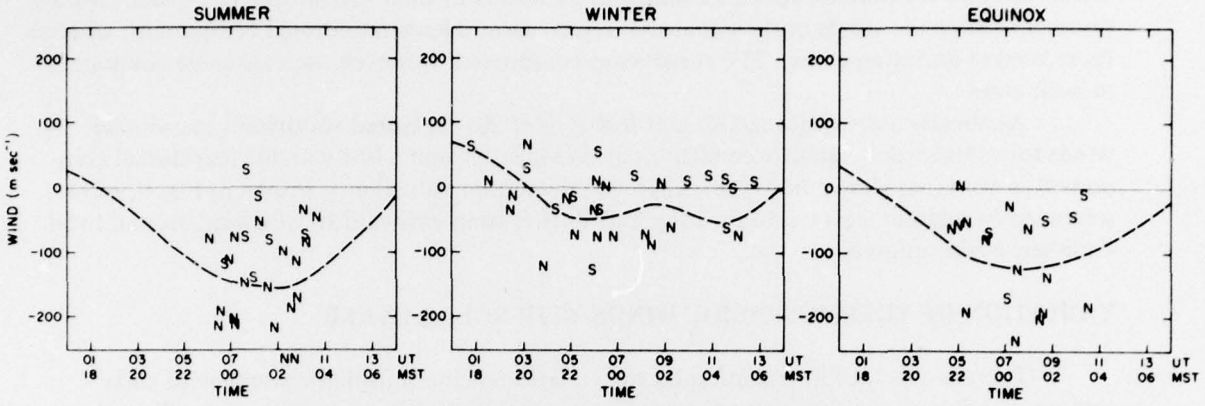

Figure 8. Meridional neutral wind measurements (m/sec) as a function of local time for summer months, winter months, and equinox months. The letters indicate the direction from Fritz Peak Observatory from which the measurements were made. The dashed line is the calculated meridional wind component determined from the thermospheric model. From Ref. 20.

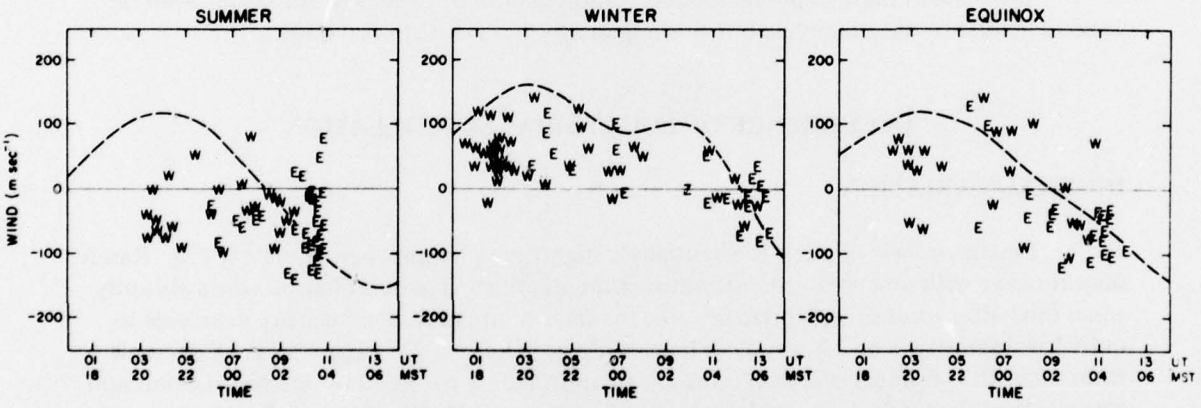

Figure 9. Same as figure 8 but for zonal winds. From Ref. 20.

SEASONAL VARIATION OF THERMOSPHERIC WINDS

There is little information available on the seasonal variation of thermospheric winds. Figures 4 and 5 show the wind patterns developed by Blum and Harris (Ref 15) for equinox conditions and for summer solstice conditions by means of their thermospheric model. During summer solstice the winds in the equatorial region show a large meridional component, whereas there is none during equinox. The zonal wind component, however, appears to be comparable in both cases.

As already stated, Hernandez and Roble (Ref 20) measured southward meridional winds for summer and equinox conditions at mid-latitude and a low variable meridional component in winter as shown in Fig. 8. Their zonal wind measurements, shown in Fig. 9, were westward in summer, eastward in winter, and shifted from eastward to westward around local midnight during equinox.

VARIATION OF THERMOSPHERIC WINDS WITH SOLAR CYCLE

There is a lack of information on the variation of thermospheric winds with solar activity. Variation of thermospheric temperature with solar activity, however, has been reported by Jacchia (Ref 9). Figure 10 shows temperature as a function of altitude for three different values of solar activity. Day-to-night differences in temperature, such as shown by Kohl and King in Fig. 11, produce density differences. These density differences cause pressure gradients, which produce the thermospheric winds (Ref 12). It would be reasonable, then, to expect higher thermospheric wind velocities during years of higher solar activity.

The various thermospheric models could possibly be evaluated for thermospheric wind dependence on solar cycle but this apparently has not yet been done.

OCCURRENCE OF EQUATORIAL SCINTILLATION

DIURNAL VARIATION

Equatorial scintillation is essentially a nighttime phenomenon (Refs 21, 22). Rarely does it occur with any great intensity during the daytime. The scintillation starts abruptly some time after local sunset, increases to a maximum intensity, then usually decreases to quite low intensity 1 or 2 hours after local midnight (Refs 1, 2). Figure 12 is an example from more than 6 hours of continuous scintillation fading recorded by the Naval Communications Area Master Station (NAVCAMS) at Guam on 30 March 1978. Full scale across the chart is more than 40 dB. Occasionally, however, the scintillation occurs in bursts, starting and stopping abruptly with periods of no scintillation as can be seen in Fig 13 for the night of 25 September 1976.

Koster (Ref 21), working in Ghana, reported that the most intense scintillations had a peak around 2200 local time. Aarons et al. (Ref 22) found similar results for their measurements made at Huancayo, Peru. Figure 14 shows their plot of diurnal occurrence of scintillation for scintillation index greater than 60. This curve also shows a peak at 2200 local time.

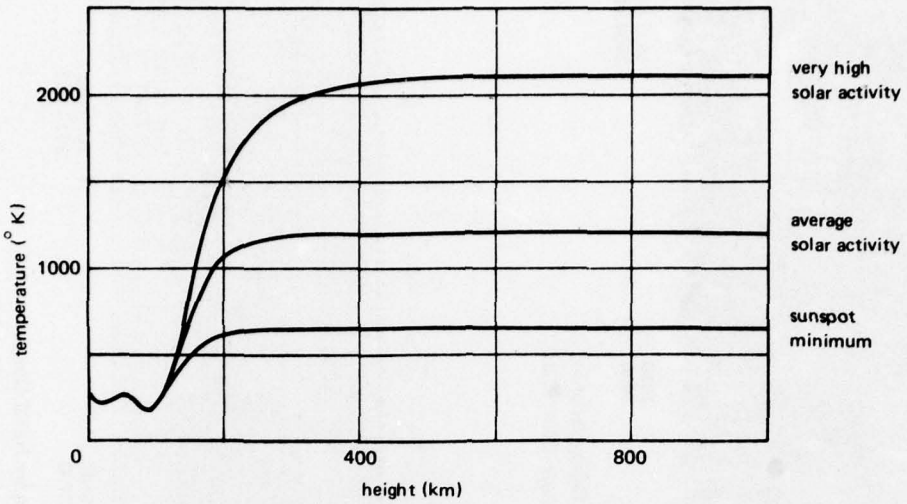

Figure 10. Atmospheric temperature profiles for three stages of solar activity. From Ref. 9.

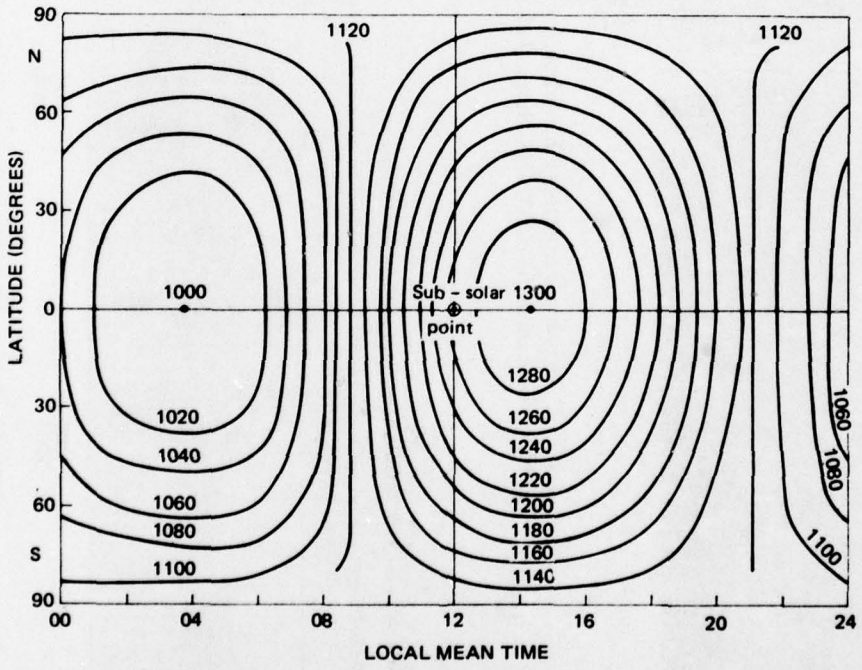

Figure 11. Equinox exospheric temperature distribution for medium solar cycle conditions, (after Jacchia, Ref. 8). From Ref. 12.

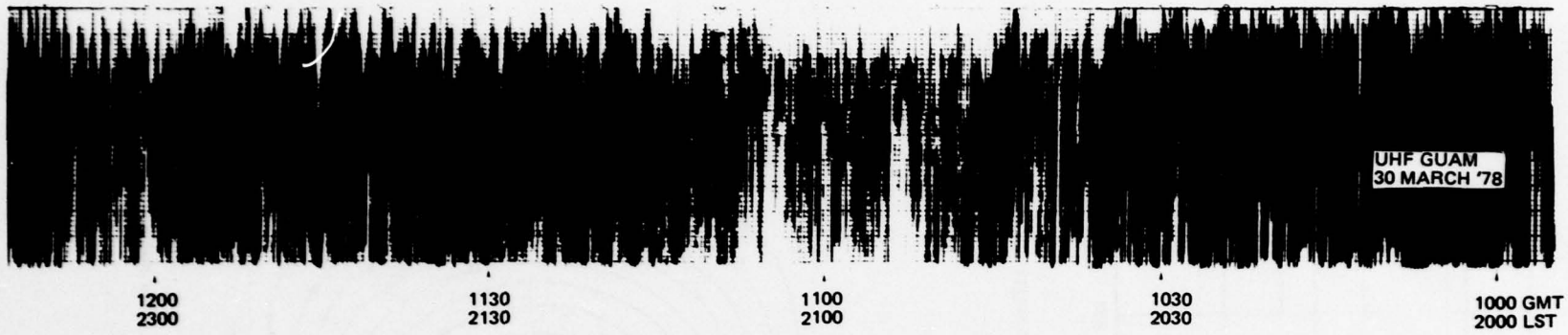

Figure 12. An example from more than 6 hours of continuous scintillation fading recorded by Navy personnel at the NAVCAMS, Guam. Full scale across the chart is more than 40 dB.

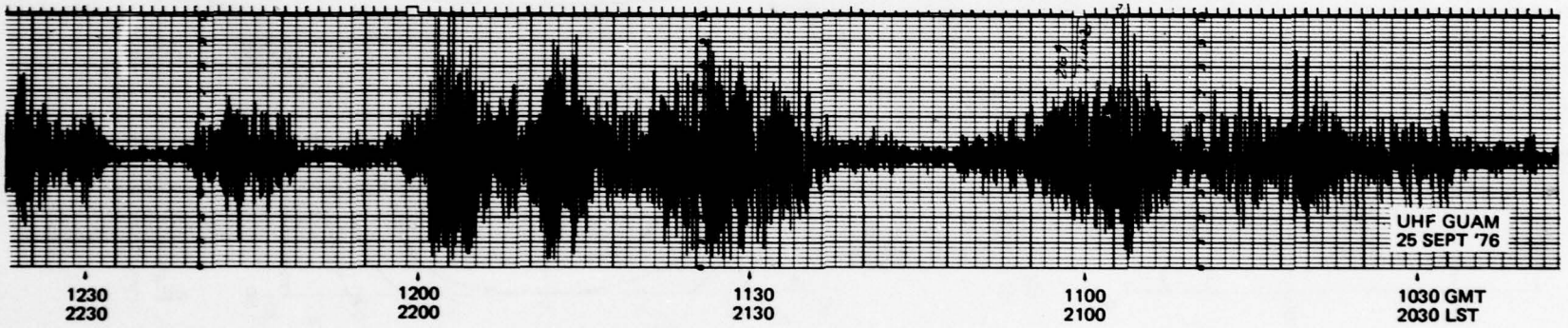

Figure 13. An example of intermittent fading recorded at NAVCAMS, Guam by Naval Ocean Systems Center personnel. Full scale across the chart is about 40 dB.

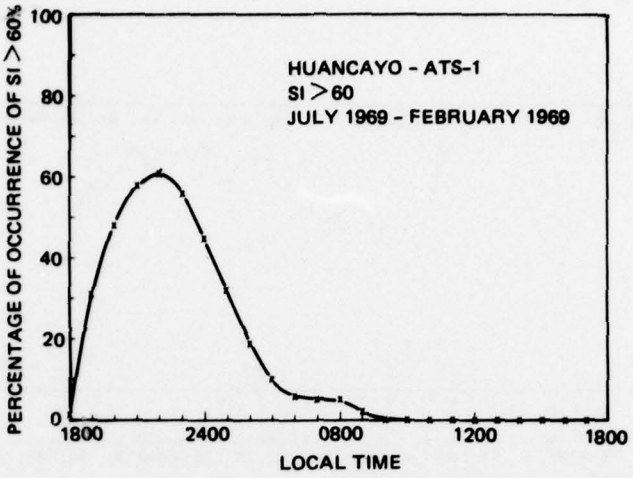

Figure 14. Diurnal occurrence of high-amplitude scintillations at Huancayo, Peru. From Ref. 22.

SEASONAL VARIATION

Equatorial scintillation does not occur every night and the duration and intensity can vary widely from night to night, particularly in years of low solar activity. Koster (Ref 21) found scintillation to be greatest at the equinoxes, with minima at the solstices. He noted, however, that the curves showed a more pronounced annual variation than a semi-annual one. Figure 15 shows his results for four successive years from 1967 to 1971. The ordinate in the plots is the nightly sum of values of a scintillation index calculated for every 5 minutes. Consequently it is a combination of the duration and the intensity of the scintillation for the night.

SOLAR-CYCLE DEPENDENCE OF EQUATORIAL SCINTILLATION

Koster (Ref 21) reported twofold dependence of equatorial scintillation on the solar cycle. The occurrence of scintillation was much greater in years of high sunspot number. In addition, the mean scintillation index during periods of scintillation was much larger near sunspot maximum than that during sunspot minimum.

Paulson and Hopkins (Ref 2), using a common 11-day period for 4 different years, plotted the occurrence of scintillation with fades greater than 6 dB against the average daily sunspot number for the 11 day period. Figure 16 shows this curve. In addition, a plot of the occurrence of scintillation against the average daily 10.7-cm flux is shown. Both curves show a very definite dependence of the occurrence of scintillation on solar activity.

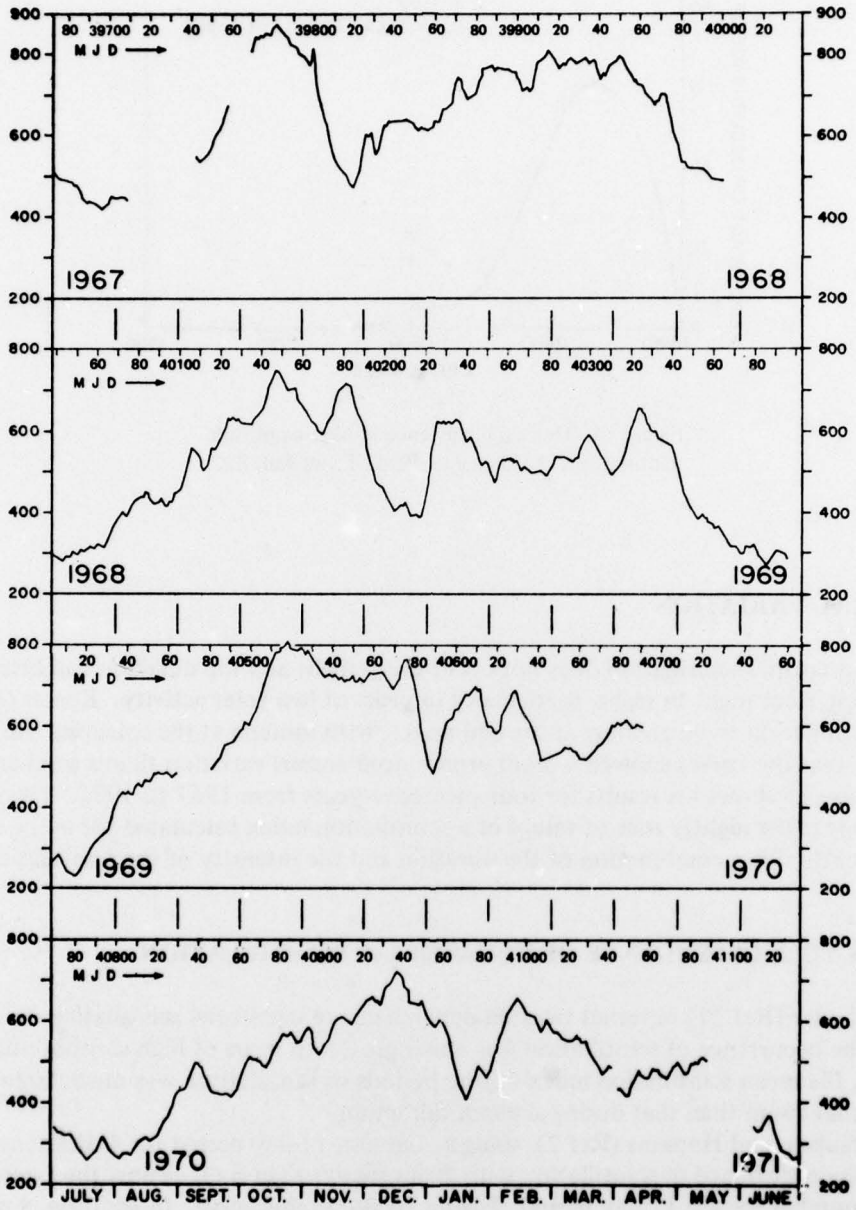

Figure 15. Smoothed seasonal variation of the sum of the nightly scintillation indices. July to June for four successive years. From Ref. 21.

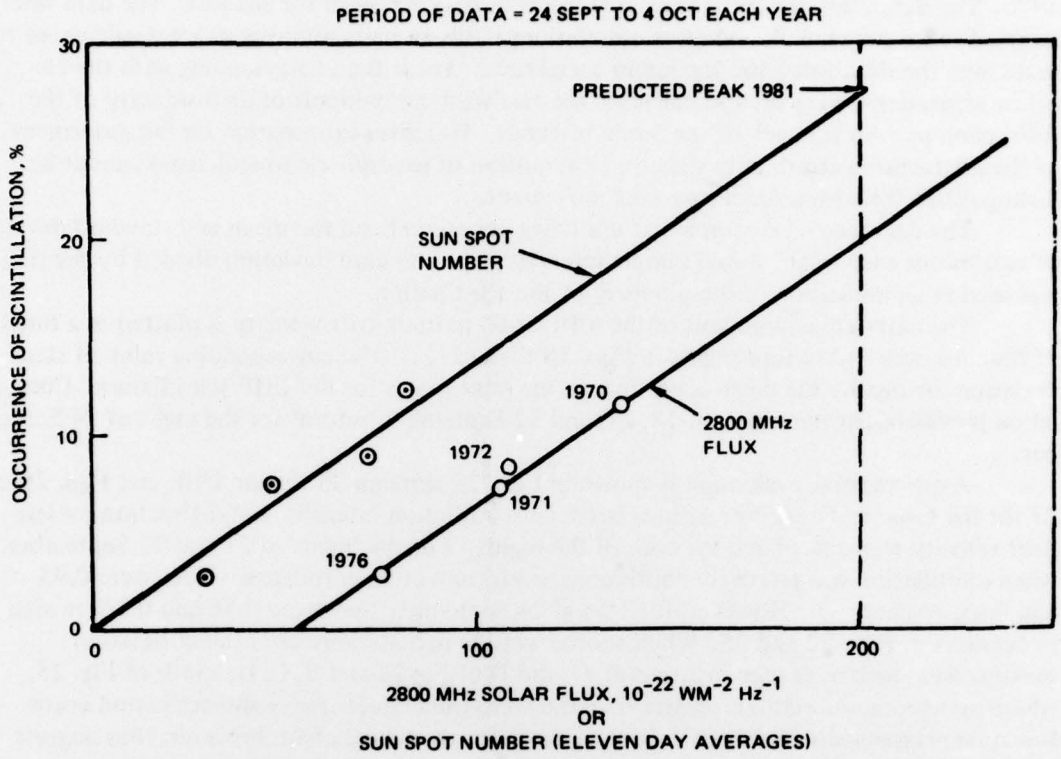

Figure 16. Dependence of scintillation occurence on solar activity.

SCINTILLATION INTENSITY VS DRIFT VELOCITY

The Naval Ocean Systems Center recorded scintillation activity at Guam during the latter half of 1976. The UHF and L-band signals at about 257 and 1541 MHz from the Pacific Gapfiller/Marisat satellite were used. During the month of September, spaced receivers were used as shown in Fig 17. Two UHF receivers were separated 1000 m in a magnetic east-west direction, with a third UHF receiver located in between at 300 m west of the east receiver. Two L-band receivers were co-located with the outer UHF receivers at the 1000-m separation. Elevation angle to the satellite was about 51 deg and azimuth was about 111 deg.

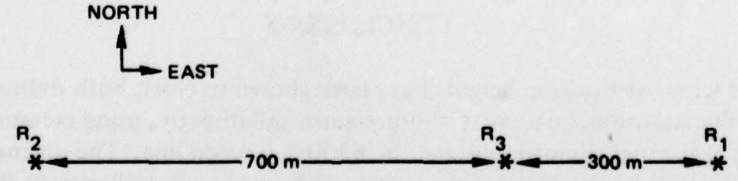

Figure 17. Dimensions and orientation of spaced receivers used at the Naval Communications Station, Guam in 1976.

Four nights of scintillation data are used in this report: 18, 21, 22, and 24 September 1976. The data were divided into sample intervals of 3 min each for analysis. The data were sampled twice per second, and cross correlations between pairs of receivers were calculated to determine the time delay for maximum correlation. These time delays, along with the receiver separations, were used to calculate the east-west components of drift velocity of the diffraction pattern for each of the 3-min intervals. This gives information on the movement of the diffraction pattern only since vertical motion of ionospheric irregularities cannot be distinguished from horizontal east-west movement.

The data were also sampled at ten times per second and the mean and standard deviation calculated for each of the 3-min sample intervals. The standard deviation divided by the mean was used as an indication of the intensity of the scintillation.

The eastward component of the diffraction pattern drift velocity is plotted as a function of time for each of the four nights in Figs. 18 through 21. The corresponding value of standard deviation divided by the mean is plotted on the same graph for the UHF scintillation. Correlation is evident for the nights of 18, 21, and 22 September but not for the night of 24 September.

A quantitative evaluation is shown in Figs. 22 through 25 for the UHF and Figs. 26 and 27 for the L-band. Cross correlations between scintillation intensity and diffraction pattern drift velocity were calculated for each of the nights. For the nights of 21 and 22 September, when scintillation was relatively continuous, maximum cross correlation values were 0.93 and 0.85, respectively. However, for 18 and 24 September they were 0.56 and 0.16, as seen in curves A in Figs. 22 and 25. When shorter sample periods were used the correlation maxima were higher, as seen in curves B, C, and D of Fig 22 and B, C, D, and E of Fig. 25, where maximum correlations greater than 0.6 were calculated. These shorter period correlations are statistically less significant than those for the whole night; however, they suggest that the reason for the low correlations for the total night might have been a varying time dependence for cases when the scintillation was intermittent. On the night of 24 September the scintillation was particularly weak and intermittent, as seen in Fig. 21.

The L-band scintillation for the nights of 21 and 22 September shows cross correlations with drift velocity for the total sample periods with maximum values of 0.82 and 0.8, respectively, as seen in curves A of Figs. 26 and 27.

The UHF results are shown in a different form in Figs. 28 through 30 for the nights of 18, 21, and 22 September. Here the scintillation intensity is plotted as a function of diffraction pattern drift velocity. The straight line in each figure is a least squares fit of the data. While the nights of 21 and 22 September are quite similar, the night of 18 September shows a much different velocity dependence. This would suggest that whereas turbulence produced by zonal winds may be causing the irregularities which produce scintillation, other factors also contribute to the intensity of the scintillation.

CONCLUSIONS

Zonal winds at F-region heights have been shown to exist, both indirectly, using models of global atmospheric density and pressure, and directly, using measurements of doppler shift in the nighttime air glow at the 6300-Å oxygen line. The diurnal variation of these zonal winds in equatorial regions shows a pronounced similarity to the nighttime variation of equatorial scintillation intensity. Seasonal and solar cycle variations in zonal winds have not been investigated in enough detail, however, to make a very meaningful comparison with the seasonal and solar cycle occurrence of equatorial scintillation.

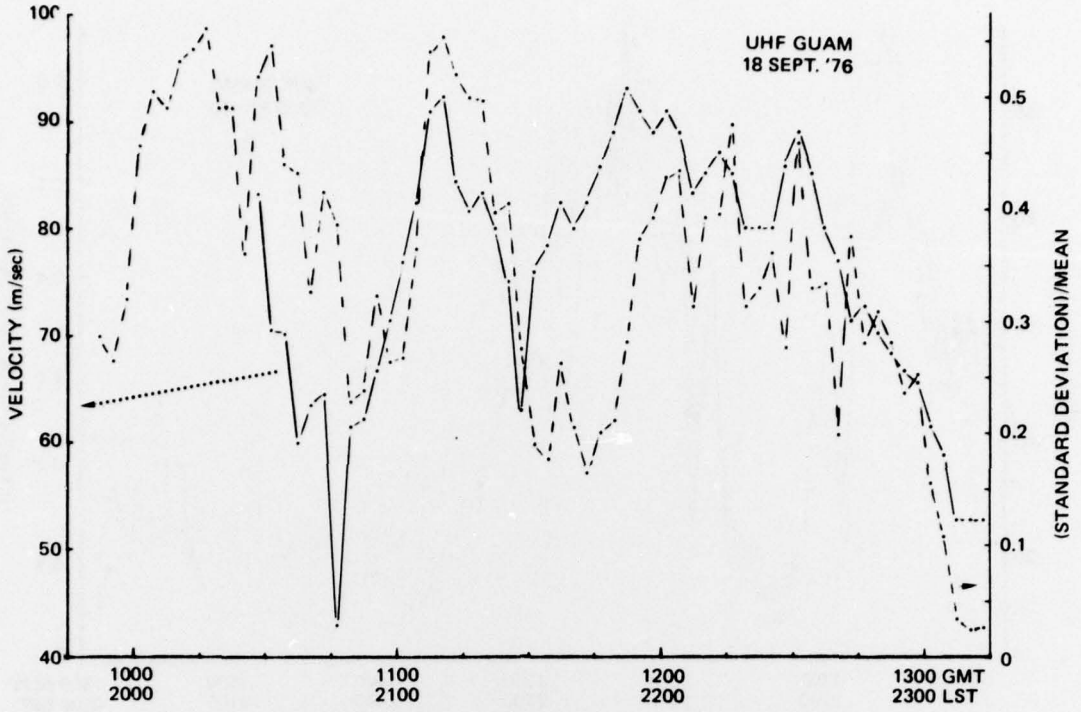

Figure 18. The eastward component of the apparent drift velocity, uncorrected for time decorrelation effects, is shown as a function of time and compared to the scintillation activity, where standard deviation divided by the mean is used as an indication of scintillation intensity.

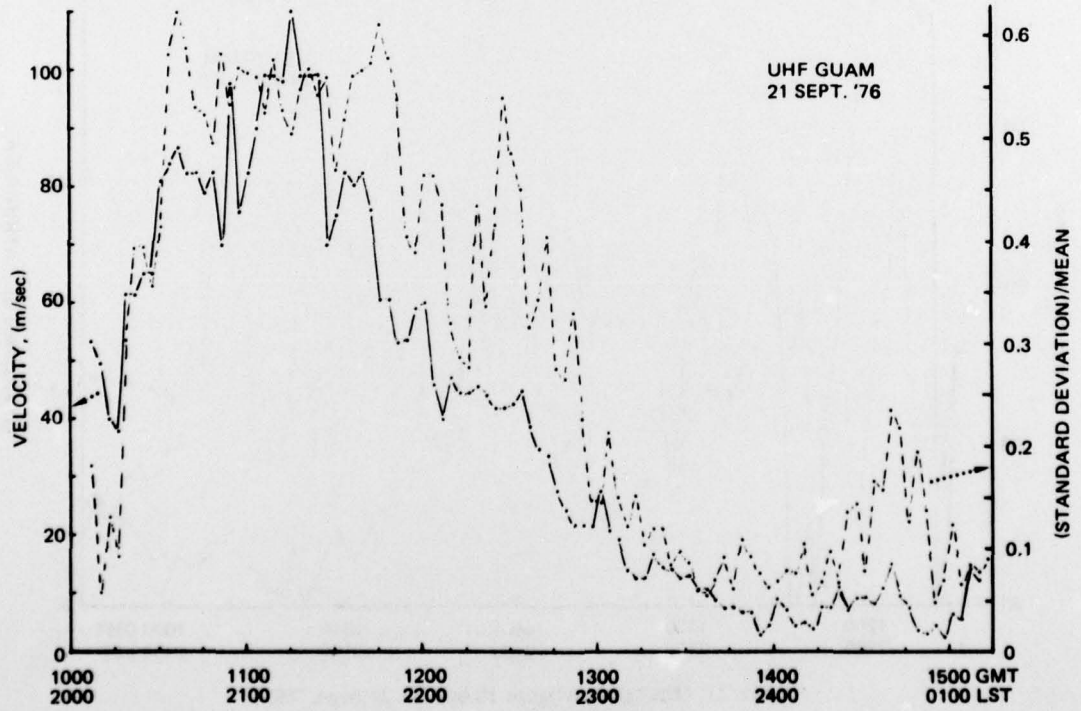

Figure 19. The same as figure 18 but for 21 Sept. '76.

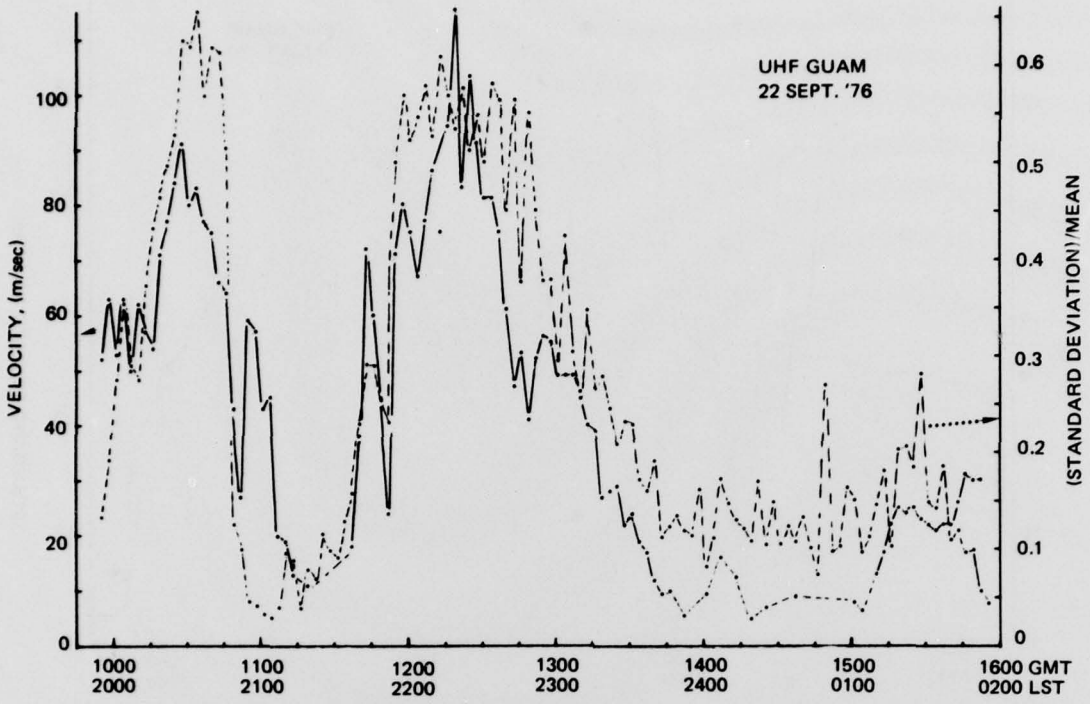

Figure 20. The same as figure 18 but for 22 Sept. '76.

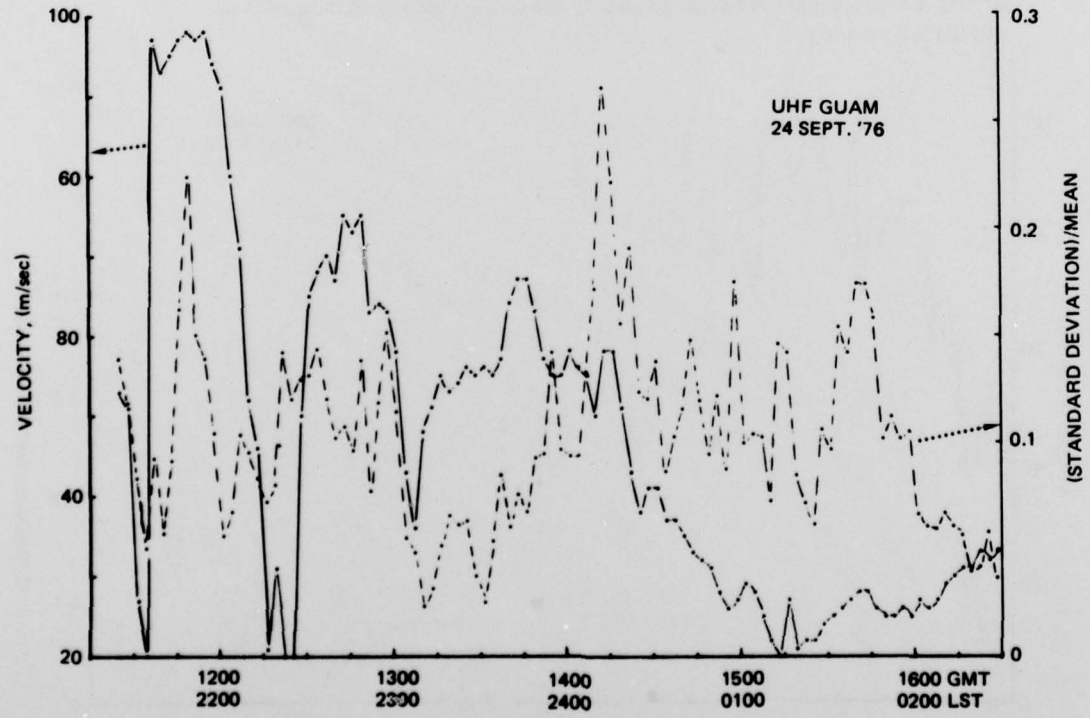

Figure 21. The same as figure 18 but for 24 Sept. '76.

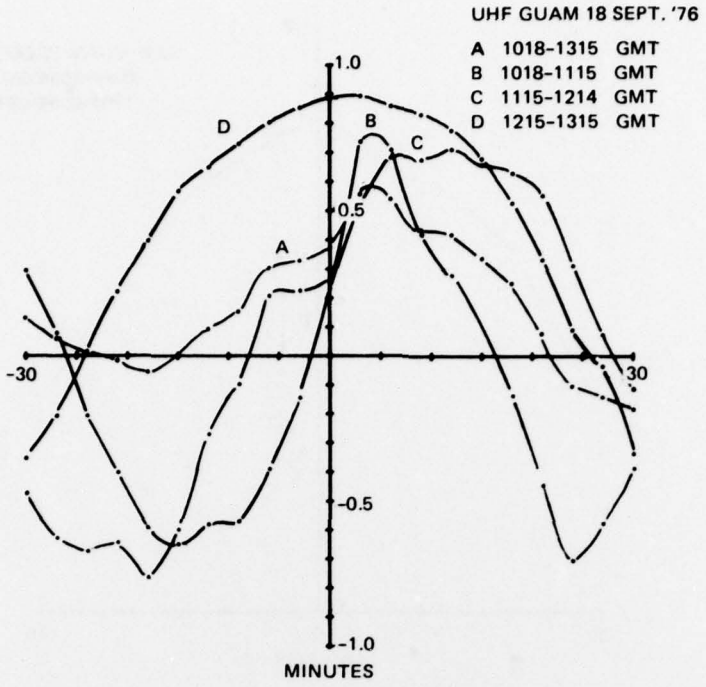

Figure 22. Correlation between diffraction pattern eastward *velocity component* and scintillation intensity.

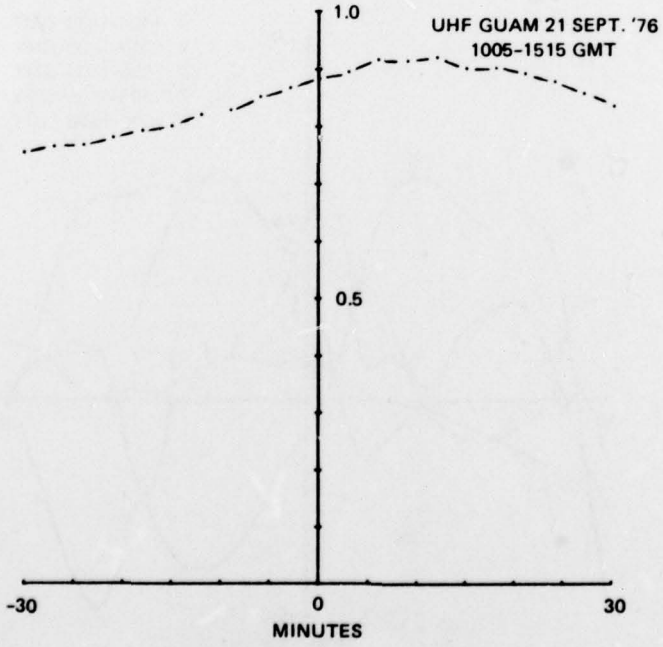

Figure 23. Correlation between diffraction pattern eastward velocity component and scintillation intensity.

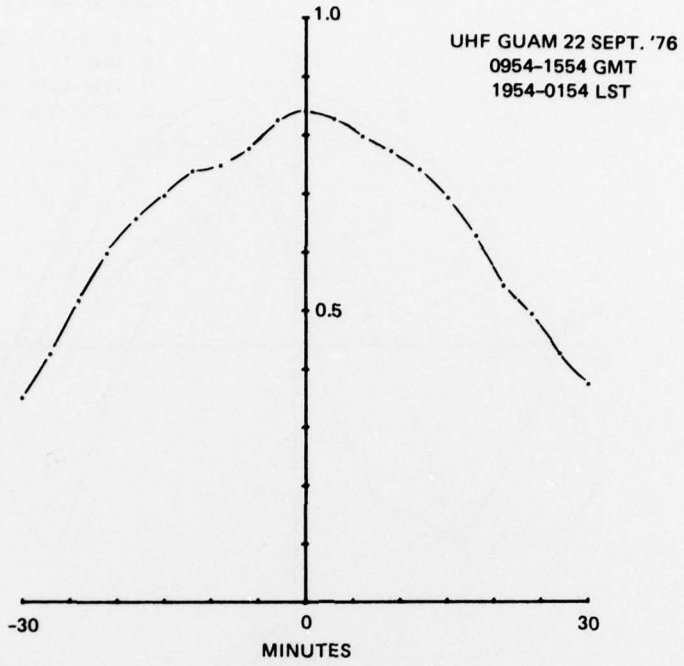

Figure 24. Correlation between diffraction pattern eastward velocity component and scintillation intensity.

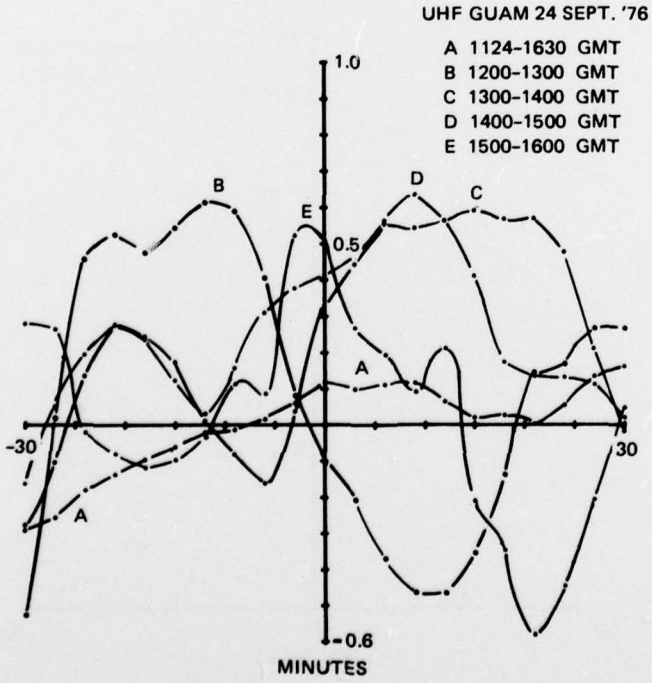

Figure 25. Correlation between diffraction pattern eastward velocity component and scintillation intensity.

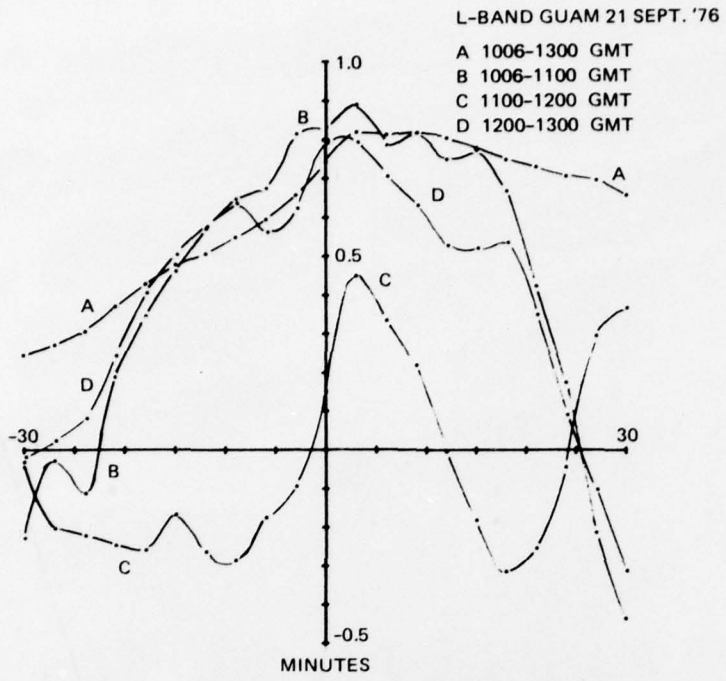

Figure 26. Correlation between diffraction pattern eastward velocity component and scintillation intensity.

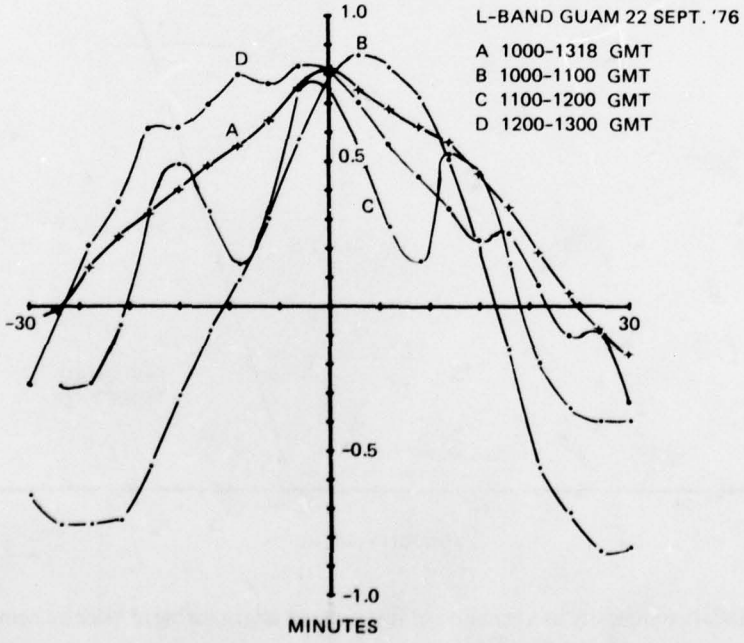

Figure 27. Correlation between diffraction pattern eastward velocity component and scintillation intensity.

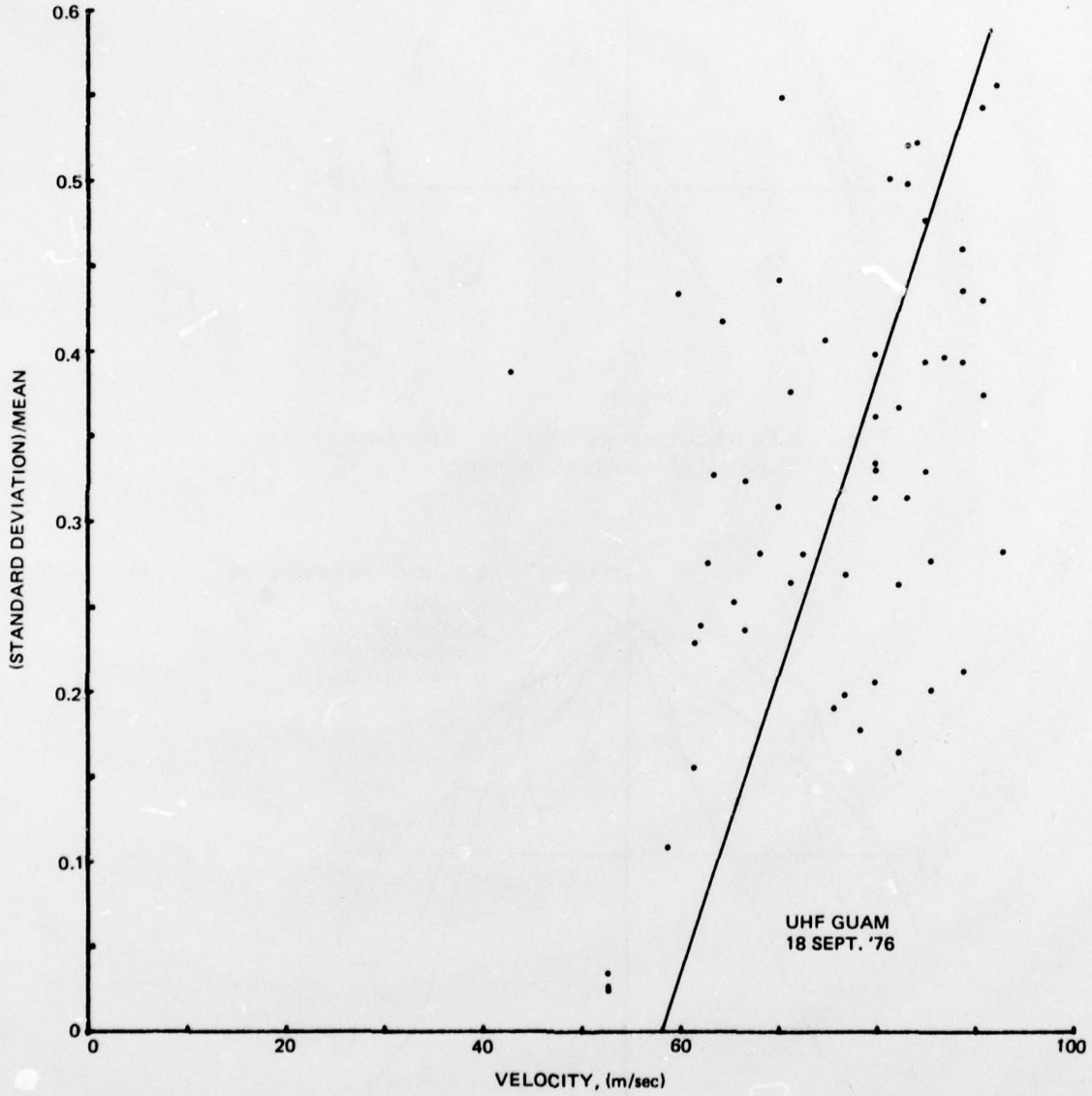

Figure 28. Scintillation intensity as a function of diffraction pattern eastward velocity component. Straight line is a least squares fit to the data.

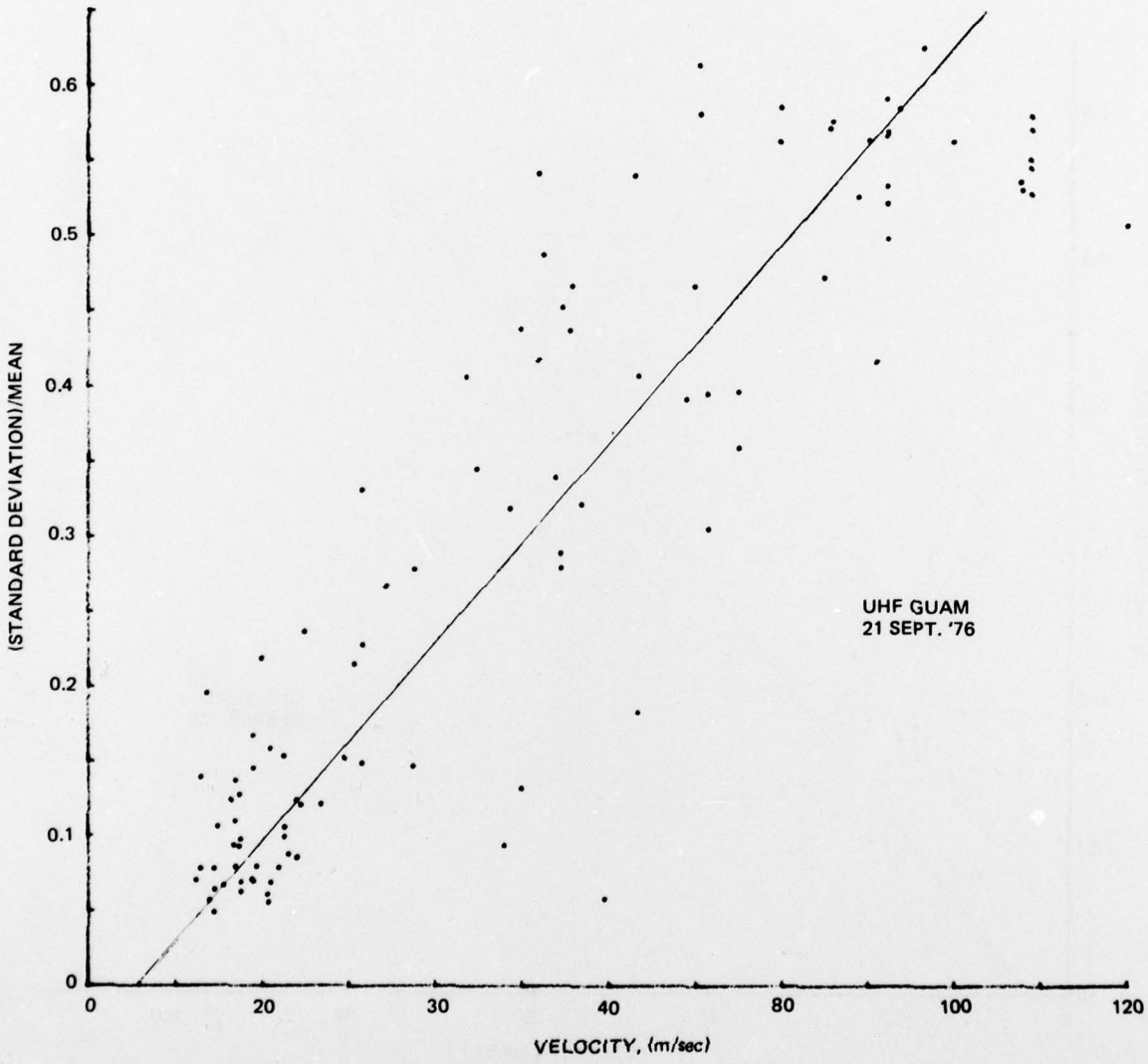

Figure 29. Scintillation intensity as a function of diffraction pattern eastward velocity component. Straight line is a least squares fit to the data.

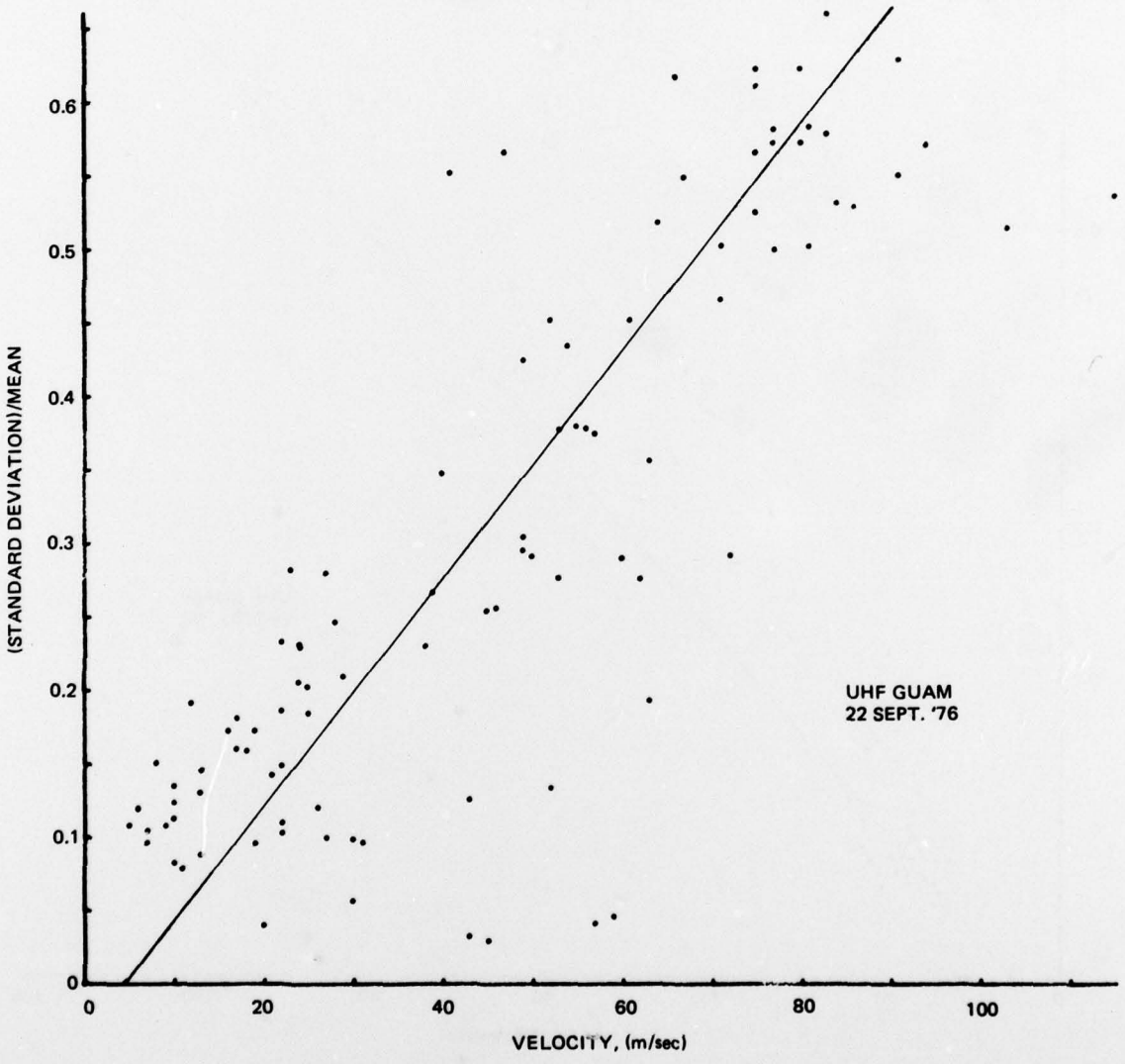

Figure 30. Scintillation intensity as a function of diffraction pattern eastward velocity component. Straight line is a least squares fit to the data.

Comparisons of scintillation intensities with diffraction pattern drift velocities show good correlation, suggesting that the irregularities in the ionospheric electron density that cause the scintillation may be generated by turbulence produced by zonal winds. Night-to-night differences in the dependence, however, would indicate that, while zonal winds may be a necessary condition for scintillation, other factors contributing to the scintillation intensity must be identified as well.

RECOMMENDATIONS

With the occurrence and the intensity of equatorial scintillation increasing as solar activity increases, additional spaced-receiver measurements should be made at both UHF and L-band frequencies to get further comparison between diffraction pattern drift velocities and scintillation intensity. The L-band measurements would be particularly useful since the scintillation at these frequencies doesn't reach saturation as soon as that at UHF.

Neutral thermospheric temperatures should also be monitored to look for a correlation between scintillation intensity and nighttime thermospheric temperatures and between zonal winds and nighttime thermospheric temperatures.

The zonal component of the neutral wind could be measured using the doppler shift of the 6300-Å oxygen line technique. Thermospheric temperatures could be determined from the doppler broadening of that same line.

These techniques would require that the measurements be made in some equatorial location where cloud cover would not be a problem.

Satellite measurements of solar radiations and particles should also be examined for periods when these measurements are made to look for solar effects which might sustain the nighttime thermospheric temperature and to look for other contributions to the scintillation intensity.

REFERENCES

1. M. R. Paulson and R. U. F. Hopkins, Effects of Equatorial Scintillation Fading on SATCOM Signals, NELC/TR 1875, 8 May 1973.
2. M. R. Paulson and R. U. F. Hopkins, Spatial Diversity Characteristics of Equatorial Scintillation, NOSC/TR 113, 2 May 1977.
3. A. Maxwell and M. Dagg, "A Radio Astronomical Investigation of Drift Movements in the Upper Atmosphere," *Phil. Mag.*, V. 45, 1954, p. 551.
4. A. Maxwell, "Turbulence in the Upper Ionosphere," *Phil. Mag.*, V. 45, 1954, p. 1247.
5. M. Dagg, "The Origin of the Ionospheric Irregularities Responsible for Radio-Star Scintillations and Spread-F – I," *J. of Atmos. and Terr. Phys.*, V. 11, 1957, p. 133.
6. M. Dagg, "The Origin of the Ionospheric Irregularities Responsible for Radio-Star Scintillations and Spread-F – II," *J. Atmos. and Terr. Phys.*, V. 11, 1957, p. 139.
7. H. Rishbeth, "Polarization Fields Produced by Winds in the Equatorial F-Region," *Planet. Space Sci.*, V. 19, 1971, p. 357.
8. L. G. Jacchia, "Static Diffusion Models of the Upper Atmosphere with Empirical Temperature Profiles," *Smith. Contr. Astrophys.*, V. 8, 1965, p. 215.
9. L. G. Jacchia, "The Upper Atmosphere," *Phil. Trans. R. Soc. Lond.*, V. A262, 1967, p. 157.
10. L. G. Jacchia, I. G. Campbell and J. W. Slowey, "A Study of the Diurnal Variation in the Thermosphere as Derived by Satellite Drat," *Planet. Space Sci.*, V. 21, 1973, p. 1825.
11. L. G. Jacchia, J. W. Slowey and I. G. Campbell, "An Analysis of the Solar-Activity Effects in the Upper Atmosphere," *Planet. Space Sci.*, V. 21, 1973, p. 1835.
12. H. Kohl and J. W. King, "Atmospheric Winds between 100 and 700 km and Their Effects on the Ionosphere," *J. Atmos. Terr. Phys.*, V. 29, 1967, p. 1045.
13. R. A. Challinor, "Neutral-Air Winds in the Ionospheric F-Region for an Asymmetric Global Pressure System," *Planet. Space Sci.*, V. 17, 1969, p. 1097.
14. L. G. Jacchia and J. W. Slowey, *Space Research*, V. 7, p. 1077, North-Holland, Amsterdam, 1967.
15. P. W. Blum and I. Harris, "Full Non-linear Treatment of the Global Thermospheric Wind System – I. Mathematical Method and Analysis of Forces," *J. Atmos. Terr. Phys.*, V. 37, 1975, p. 193.
16. P. W. Blum, and I. Harris, "Full Non-linear Treatment of the Global Thermospheric Wind System – II. Results and Comparison with Observations," *J. Atmos. Terr. Phys.*, V. 37, 1975, p. 213.
17. J. S. Nisbet, Ionospheric Research Scientific Report No. 355, Pennsylvania State University, 1970, Unpublished.
18. R. G. Roble, B. A. Emery, J. E. Salah, and P. B. Hays, "Diurnal Variation of the Neutral Thermospheric Winds Determined from Incoherent Scatter Radar Data," *J. Geophys. Res.*, V. 79, 1974, p. 2808.

REFERENCES (Continued)

19. E. B. Armstrong, "Doppler Shifts in the Wavelength of the OI 6300 Line in the Night Airglow," *Planet. Space Sci.*, V. 17, 1969, p. 957.

20. G. Hernandez and R. G. Roble, "Direct Measurement of Nighttime Thermospheric Winds and Temperatures, 1. Seasonal Variations During Geomagnetic Quiet Periods," *J. Geophys. Res.*, V. 81, 1976, p. 2065.

21. J. R. Koster, "Equatorial Scintillation," *Planet. Space Sci.*, V. 20, 1972, p. 1999.

22. J. Aarons, H. E. Whitney and R. S. Allen, "Global Morphology of Ionospheric Scintillation," *Proc. IEEE*, V. 59, 1971, p. 159.